

Transport properties of hydrogen-doped $(\text{Zr}_{80}\text{3d}_{20})_{1-x}\text{H}_x$ ($3d = \text{Co}, \text{Ni}$) metallic glasses

I. Kokanović^{*1}, B. Leontić¹, and J. Lukatela²

¹ Department of Physics, Faculty of Science, University of Zagreb, 10 000 Zagreb, Croatia

² Institute of Physics, 10 000 Zagreb, Croatia

Received 4 September 2003, revised 26 November 2003, accepted 2 December 2003

Published online 4 February 2004

PACS 74.70.Ad, 75.47.Np, 81.05.Kf

The electrical resistivities of hydrogen-doped $(\text{Zr}_{80}\text{3d}_{20})_{1-x}\text{H}_x$ ($3d = \text{Ni}, \text{Co}; x \leq 0.11$) metallic glasses have been measured at temperatures between 2 K and 110 K and in magnetic fields up to 1 T for various dopant concentrations. These systems have a high room-temperature resistivity ($\rho > 160 \mu\Omega \text{ cm}$) and become superconducting below 4 K. The increase of the room-temperature resistivity and its temperature coefficient with hydrogen dopant concentration is explained as due to an increase of disorder with hydrogen-doping. The temperature and magnetic field dependence of the resistivity has been analysed using theoretical models of weak-localisation and electron–electron interaction in disordered conductors. The hydrogen dopant is found to reduce the effective electron diffusion constant, D , the spin-orbit scattering rate, τ_{so}^{-1} , the superconducting transition temperature, T_c , and broadens the superconducting transition region. The contribution of the Maki-Thompson interaction to the magnetoresistivity is also reduced.

© 2004 WILEY-VCH Verlag GmbH & Co. KGaA, Weinheim

1 Introduction

Metallic glasses offer an excellent matrix in which to study the behaviour of electrons in disordered systems. It has been shown that the diffusive motion of electrons in two-dimensional as well as in three-dimensional disordered systems entails quantum corrections to the resistivity and magnetoresistivity. There are two principal sources of quantum corrections, known as weak localisation, WL, [1, 2] and Coulomb interaction, CI, [3, 4]. Both of these corrections are important when the mean free path becomes short so that electron propagation between scattering events is no longer free-electron-like but diffusive. At low enough temperatures, where the elastic scattering time is a few orders of magnitude shorter than the inelastic scattering time, the quantum corrections arising from the interference of the electronic partial waves are very important. It has been shown that constructive interference of the electronic waves can only be expected in a back-scattering geometry, thus producing an increase of the sample resistivity. The magnitude of this additional contribution at a given temperature is reduced by the presence of the inelastic, spin-orbit or spin-flip scattering, since they destroy the constructive interference. An external magnetic field also causes dephasing of partial waves generating a particular behaviour in magnetoresistivity. The diffusive character of electrons in highly disordered materials also leads to a reduced screening of the electron–electron interaction.

The quantum corrections lead to an anomalous dependence of the resistivity on temperature, sample dimension, and external fields [5–8]. Although the WL and CI theories have been developed for free electrons, their applicability to transition-element metallic glasses, with dominant d-band conductivity, has been successful.

* Corresponding author: e-mail: kivan@phy.hr, Phone: +385 1 460 5551, Fax: +385 1 468 0336

We report on the resistive properties resulting from doping $Zr_{80}3d_{20}$ ($3d = Ni, Co$) metallic glasses with hydrogen. These glasses are characterised by high room-temperature resistivities, they are paramagnetic and become superconducting at temperatures below 4 K. The hydrogen dopant, as used here, plays the role of an atomic probe to study quantum interference at defects and to gain insight into the way the atomic microenvironment influences the electronic properties of the disordered system.

2 Experimental methods

Ribbons of $Zr_{80}3d_{20}$ metallic glass were prepared by rapid solidification of the melt on a single-roll spinning copper wheel in an argon atmosphere. The samples, 1–2 cm long, 1.5 mm wide and 25 μm thick were then cut from the ribbon. The hydrogenation was carried out electrolytically. The amount of absorbed hydrogen was determined volumetrically. The as-quenched and hydrogenated samples were examined by X-ray diffraction, using $\text{Cu K}\alpha$ radiation to verify that they were amorphous.

The sample resistance was measured by a low-frequency (23.2 Hz) four-probe ac method in the temperature range 2–290 K and in magnetic fields up to 1 T. The precision of these measurements extends to a few parts in 10^6 . The temperature range from 2–40 K was covered using a liquid-helium cryostat, while, above 40 K and up to 290 K, the measurements were carried out in a Cryodyne Refrigerator.

3 Theoretical models

In a superconductor, the fluctuating conductivity dominates over the localisation and CI conductivity in the vicinity of the superconducting transition temperature, T_c . This excess electrical conductivity consists of two terms

$$\Delta\sigma = \sigma_{\text{AL}} + \sigma_{\text{MT}}, \quad (1)$$

where σ_{AL} is the Aslamazov–Larkin, (AL) [9], term, which originates from the virtual Cooper pairs created by thermal fluctuations and σ_{MT} is the Maki–Thompson, (MT) [10], term, coming from the interaction of normal conducting electrons and the superfluid.

In three dimensions, the temperature-dependent quantum correction to the conductivity due to WL in the presence of inelastic, τ_i , and spin-orbit, τ_{so} , scattering is given by Fukuyama and Hoshino [1] as

$$\sigma_{\text{WL}} = \frac{e^2}{2\pi^2\hbar} \left[3 \left(\frac{1}{D\tau_{\text{so}}} + \frac{1}{4D\tau_i} \right)^{1/2} - \left(\frac{1}{4D\tau_i} \right)^{1/2} \right], \quad (2)$$

where D is the diffusion coefficient. τ_{so} is temperature independent and $\tau_i = \alpha_i T^{-p}$, with $2 \leq p \leq 4$ at temperatures $T < \Theta_D$ (Θ_D is the Debye temperature), at which the dominant contribution to the inelastic scattering comes from the electron–phonon interaction.

The correction for the electron–electron interaction in the diffusion and the Cooper channels takes the following form [3, 4]

$$\sigma_{e-e} = \frac{1.3e^2}{4\pi^2\hbar} \left(\frac{4}{3} - 3F^* - \frac{2}{\ln(T_0/T)} \right) \left(\frac{kT}{D\hbar} \right)^{1/2}, \quad (3)$$

where T_0 is equal to T_c , if the alloy is a superconductor. Otherwise, T_0 is taken to be of the order of the Fermi temperature, T_F . $F^* = F - \lambda$, where F is the averaged screened Coulomb potential ($0 \leq F \leq 1$, depending on the screening length) and λ is the electron–phonon coupling constant.

The complete magnetoresistivity expression due to the weak localisation, superconducting fluctuations (the Maki–Thompson contribution), the spin-orbit scattering, the spin Zeeman, and the orbital effects has

been developed by Fukuyama and Hoshino and is given by [1], and [11] as

$$\Delta\rho = \rho(B, T) - \rho(0, T) = -A\rho^2 \{u^{1/2} [F_3((1+t)/u) - \beta F_3(t/u)] + 0.5(u/(1-\gamma))^{1/2} [F_3(t_+/u) - F_3(t_-/u)] - (t_-^{1/2} - t_+^{1/2})/(1-\gamma)^{1/2} + t^{1/2} - (t+1)^{1/2}\}, \quad (4)$$

with $A = e^2(D\tau_{so})^{-1/2}/2\pi^2\hbar$, $\gamma = [g^*\mu_B B \tau_{so}/2\hbar(1-I)]^2$, $u = eDB\tau_{so}/\hbar$, $t = \tau_{so}/4\tau_i$, $t_{\pm} = t + 0.5 [1 \pm (1-\gamma)^{1/2}]$, and

$$F_3(z) = \sum \{2[(n+z+1)^{-1/2} - (n+z)^{-1/2}] - (n+z+0.5)^{-1/2}\},$$

where $D = v_F^2 d/3$ is the diffusion constant; τ , τ_i , and τ_{so} are the elastic, the inelastic, and the spin-orbit scattering times, respectively; g^* is the effective g factor, $(1-I)^{-1}$ is the Stoner factor, and μ_B is the Bohr magneton. The term proportional to β arises from the Maki-Thompson interaction. The magnetic field dependence of the Maki-Thompson fluctuation conductivity was first discussed by Larkin [12] who derived an expression valid in the low-field limit, for temperatures not too close to T_c . After calculating $g(T)^{-1} = \ln(T_c/T)$ we use Larkin's tabulation to obtain $\beta(T)$.

The contributions to the magnetoresistivity arising from the Coulomb interaction are the orbital effects in the Cooper channel [2]

$$\Delta\rho = \rho^2 g(T, B) e^2/(8\pi^2\hbar) (eB/\hbar)^{1/2} \Phi_3(2DeB/\pi k_B T), \quad (5)$$

and the spin splitting of the conduction electron energies in the diffusion channel [3]

$$\Delta\rho = \rho^2 e^2/(4\pi^2\hbar) F^*(k_B T/2\hbar D)^{1/2} g_3(g\mu_B B/k_B T), \quad (6)$$

with

$$F^* = 32F/3 [(1+F/2)^{3/2} - (1+3F/4)],$$

where F is the averaged screened Coulomb potential ($0 \leq F \leq 1$, depending on the screening length), the functions Φ_3 , g_3 are similar in form to F_3 .

4 Results and discussion

The change in the temperature-dependent electrical resistivity, relative to its value at 290 K, $\Delta\rho/\rho(290 \text{ K})$, of hydrogen-doped $(\text{Zr}_{80}\text{Ni}_{20})_{1-x}\text{H}_x$ ($x = 0, 0.03, 0.05, 0.11$) and $(\text{Zr}_{80}\text{Co}_{20})_{1-x}\text{H}_x$ ($x = 0, 0.015, 0.05, 0.11$) samples for temperatures $3 \text{ K} < T < 110 \text{ K}$ are shown in Fig. 1 and 2, respectively. The solid lines are the best fits to the sum of Eq. (2, 3). The temperature coefficients of the resistivity (TCR) of the hydrogen-doped $(\text{Zr}_{80}\text{3d}_{20})_{1-x}\text{H}_x$ (3d = Co, Ni) samples are negative above 10 K and their absolute values increase with the hydrogen concentration.

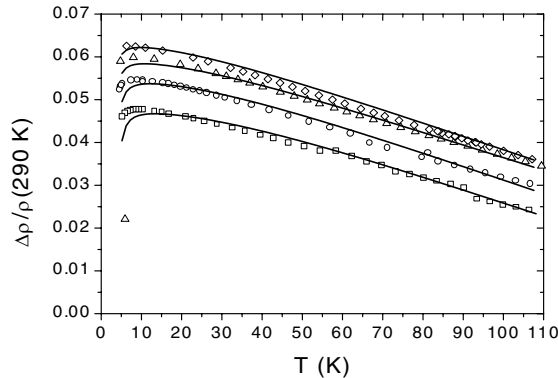


Fig. 1 Change in the temperature-dependent electrical resistivity, relative to its value at 290 K, of hydrogen doped $(\text{Zr}_{80}\text{Ni}_{20})_{1-x}\text{H}_x$ metallic glasses. [$x = 0$ (\square), 0.03 (\circ), 0.05 (Δ), 0.11 (\diamond)]. The lines are the best fits to the sum of Eq. (2) and (3).

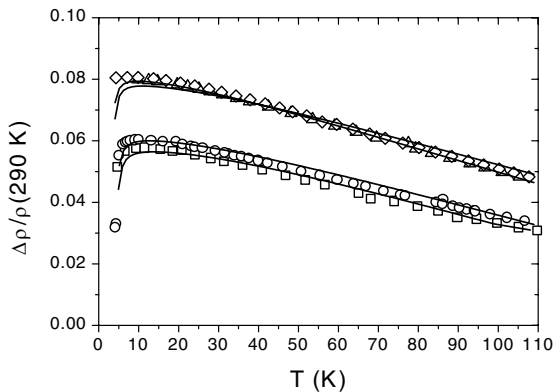


Fig. 2 Change in the temperature-dependent electrical resistivity, relative to its value at 290 K, of hydrogen doped $(\text{Zr}_{80}\text{Co}_{20})_{1-x}\text{H}_x$ metallic glasses. [$x = 0$ (\square), 0.015 (\circ), 0.05 (Δ), 0.11 (\diamond)]. The lines are the best fits to the sum of Eq. (2) and (3).

The temperature-dependent part of the electrical resistivity relative to its value at 4.2 K, $\rho(T)/\rho(4.2 \text{ K})$, of $(\text{Zr}_{80}\text{Ni}_{20})_{1-x}\text{H}_x$ metallic glasses ($x = 0, 0.03, 0.05, 0.11$), in the vicinity of T_c is shown in Fig. 3. Doping with hydrogen reduces T_c , the superconducting transition region broadens and “steps” appear in the resistance curve at the transition for hydrogen concentration $x = 0.11$.

These steps can be associated with inhomogeneities due to different environments of H-atoms in the matrix. According to the structural analyses of hydrogen doped Zr-3d metallic glasses [13] H-atoms tend to occupy preferentially tetrahedral holes surrounded by four Zr-atoms. If we compare the present results with our earlier investigation of $(\text{Zr}_{67}\text{Co}_{33})_{1-x}\text{H}_x$ metallic glasses [14], we conclude that, in the system with higher zirconium concentration, the “steps” appear at a higher hydrogen concentration. Hydrogen atoms thus migrate to the Zr-rich sites where their s -electron hybridise with Zr d -band. This results in a reduction of the Zr 4d-density of states at E_F . The same effect has been observed in the low-temperature specific heat measurements of hydrogen-doped Zr-Ni metallic glasses [15]. Thus we can conclude that the lowering of T_c is due to the decrease of the Zr 4d-density of states at the Fermi level and an enhancement of the system disorder with increasing hydrogen concentration.

The magnetoresistivity of $(\text{Zr}_{80}\text{Ni}_{20})_{1-x}\text{H}_x$ metallic glass as a function of magnetic fields up to 1 T, for various hydrogen concentrations ($x = 0, 0.03, 0.05, 0.11$) is shown in Fig. 4. The magnetoresistivity is positive for all samples. The increase of hydrogen concentration leads to a decrease of the magnetoresistance slopes, and hence of the Maki–Thompson contribution and T_c . The magnetoresistivity of $(\text{Zr}_{80}\text{Co}_{20})_{0.95}\text{H}_{0.05}$ sample as a function of magnetic fields up to 1 T, for various temperatures, T , ($T = 4.19 \text{ K}, 5 \text{ K}$ and 6 K) is shown in Fig. 5. The increase of temperature leads also to a decrease of the magnetoresistance slopes, and hence of the Maki–Thompson contribution.

The temperature-dependent change of the resistivity of $(\text{Zr}_{80}\text{Ni}_{20})_{1-x}\text{H}_x$ metallic glasses consists of two contributions: weak localisation and electron–electron interaction. The fits to the experimental data (Fig. 1, 2) are derived from the sum of relations (2) and (3) with the inelastic scattering time,

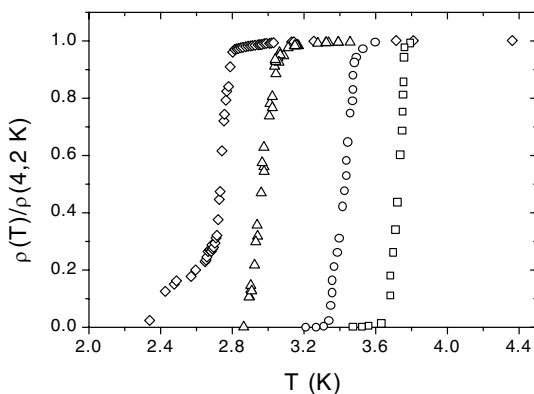


Fig. 3 The temperature-dependent part of the electrical resistivity relative to its value at 4.2 K, $\rho(T)/\rho(4.2 \text{ K})$, of $(\text{Zr}_{80}\text{Ni}_{20})_{1-x}\text{H}_x$ metallic glasses [$x = 0$ (\square), 0.03 (\circ), 0.05 (Δ), 0.11 (\diamond)].

Table 1 Values of the hydrogen concentration, x , the diffusion constant, D , the inelastic scattering time, τ_i (4.2 K), the spin-orbit scattering time, τ_{so} , the superconducting transition temperature, T_c , the electrical resistivity, ρ (290 K), and the screening parameter F^* , obtained from the resistivity data.

| x | D | τ_i (4.2 K) | τ_{so} | T_c | ρ (290 K) | F^* |
|--|--|------------------------------------|------------------------------------|-----------------|-----------------------------------|------------|
| ± 0.002 | ± 0.02 $10^{-5} \text{ m}^2 \text{ s}^{-1}$ | ± 0.02 10^{-11} s | ± 0.02 10^{-13} s | ± 0.02 K | ± 1 $\mu\Omega \text{ cm}$ | ± 0.03 |
| $(\text{Zr}_{80}\text{Ni}_{20})_{1-x}\text{H}_x$ | | | | | | |
| 0 | 3 | 0.95 | 3.5 | 3.72 | 165 | 0.1 |
| 0.03 | 2.97 | 0.96 | 4.5 | 3.42 | 168 | 0.1 |
| 0.05 | 2.94 | 1.27 | 6.5 | 2.97 | 173 | 0.1 |
| 0.11 | 2.85 | 1.36 | 8.0 | 2.72 | 183 | 0.1 |
| $(\text{Zr}_{80}\text{Co}_{20})_{1-x}\text{H}_x$ | | | | | | |
| 0 | 3 | 0.79 | 3.5 | 3.98 | 170 | 0.1 |
| 0.015 | 2.95 | 0.96 | 4.5 | 3.87 | 173 | 0.03 |
| 0.05 | 2.9 | 1.03 | 5.2 | 3.24 | 177 | 0.03 |
| 0.11 | 2.8 | 1.08 | 7.5 | 2.98 | 188 | 0.03 |

$\tau_i = \alpha_i T^{-2}$, the spin-orbit scattering time, τ_{so} , the diffusion constant, D , and the screening parameter, F^* , used as the fitting parameters. The values of the parameters are given in Table 1. The values of T_c and ρ (290 K) are those determined experimentally. T_c is taken as the midway point on the electrical resistivity vs. temperature transition curve. The influence of the changes in the value of parameters to the fitting procedure is considerable. Thus, for example, a change of 5% in only one of the parameters D , τ_i and τ_{so} gives a fit, which deviates significantly from the experimental data.

We can conclude that the quantum corrections to the resistivity are proportional to $T^{1/2} \ln^{-1}(T_c/T)$ from 4 K to 20 K as predicted by the electron–electron interaction model (Eq. 3) and to $-T$ from 20 K to 110 K due to weak localisation.

It can be seen from Table 1 that the diffusion constant, D , decreases with the increase of hydrogen concentration in the $(\text{Zr}_{80}3\text{d}_{20})_{1-x}\text{H}_x$ (3d = Ni, Co) system. The inelastic scattering time, τ_i , increases in $(\text{Zr}_{80}3\text{d}_{20})_{1-x}\text{H}_x$ (3d = Ni, Co), (Table 1).

If we calculate the inelastic phase coherence length, $L_i(T) = \sqrt{D \cdot \tau_i}$, we find that it increases from $L_i^{\text{Ni}}(4.2 \text{ K}) = 1.69 \times 10^{-8} \text{ m}$, $L_i^{\text{Co}}(4.2 \text{ K}) = 1.54 \times 10^{-8} \text{ m}$ in the undoped samples $\text{Zr}_{80}3\text{d}_{20}$ (3d = Ni, Co) to $L_i^{\text{Ni}}(4.2 \text{ K}) = 1.97 \times 10^{-8} \text{ m}$, $L_i^{\text{Co}}(4.2 \text{ K}) = 1.74 \times 10^{-8} \text{ m}$ in the doped samples $(\text{Zr}_{80}3\text{d}_{20})_{0.89}\text{H}_{0.11}$. This implies that the weak-localisation correction increases with hydrogen, while the screening parameter F^* in the electron–electron contribution is constant ($F^{*(\text{Ni, Co})} \approx 0.1$ in Table 1).

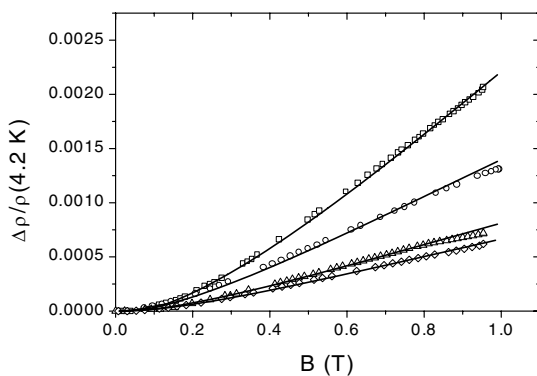


Fig. 4 Change in the magnetoresistivity relative to the resistivity at $T = 4.2 \text{ K}$, $\Delta\rho/\rho(4.2 \text{ K})$, versus magnetic field, $B(T)$, of hydrogen doped $(\text{Zr}_{80}\text{Ni}_{20})_{1-x}\text{H}_x$ metallic glasses (\square - $x = 0$; \circ - $x = 0.03$; Δ - $x = 0.05$; \diamond - $x = 0.11$). Solid lines are the best fits to the sum Eq. (4–6).

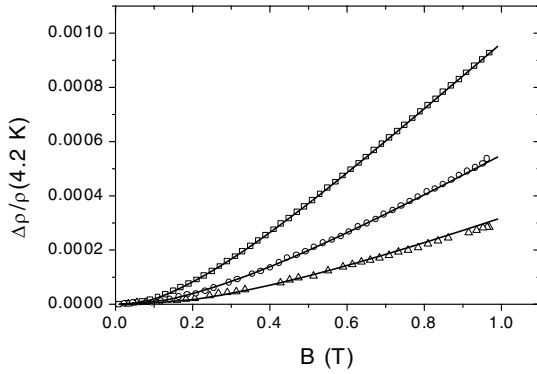


Fig. 5 Change in the magnetoresistivity relative to the resistivity at $T = 4.2$ K, $\Delta\rho/\rho(4.2$ K), versus magnetic field, $B(T)$, of hydrogen doped $(\text{Zr}_{80}\text{Co}_{20})_{0.95}\text{H}_{0.05}$ metallic glasses at $T = 4.19$ K (\square), 5 K (\circ) and 6 K (Δ). Solid lines are the best fits to the sum Eq. (4–6).

The spin-orbit scattering time, τ_{so} , is enhanced with increased hydrogen concentration (Table 1). Since most of the spin-orbit scattering takes place on Zr atoms and in the d-band, the reduction of the effective spin-orbit contribution to the resistivity by the dopant can be taken also as evidence that hydrogen atoms migrate mainly to the Zr-rich sites.

The electrical resistivity in hydrogen doped $(\text{Zr}_{80}\text{3d}_{20})_{1-x}\text{H}_x$ systems increases with hydrogen concentration (Table 1). We have found that sample dimensions remain unchanged during hydrogenation thus, the error of the resistivity in Table 1 is in fact the error of the measured resistance and does not include the error due to the geometrical factor, which remains unchanged during the measurements. In the case of strong scattering, the electron motion becomes diffusive so that the resistivity is expressed as $\rho = (e^2 N(E_F) D)^{-1}$. The values of the density of states at Fermi level, $N(E_F)$, derived from the relation, $N(E_F) = (e^2 \rho D)^{-1}$, are given in Table 2. Hydrogen reduces the d-density of states at the Fermi-level in Zr-3d metallic glasses, which is consistent with the ultra-violet photoelectron spectroscopy measurements [16] as well as the magnetic susceptibility results [17] and specific heat measurements [15]. Thus we conclude that the resistivity increase of $(\text{Zr}_{80}\text{3d}_{20})_{1-x}\text{H}_x$ (3d = Co, Ni), (Table 1), is partly caused by the decrease of the density of d-states at the Fermi level, $N(E_F)$, and partly by the observed decrease of the electron diffusion constant, D , (Table 1).

The solid curves fitted to the experimental magnetoresistivity data in Fig. 4 and 5 are derived from the sum of relations (4–6) with the inelastic scattering time, τ_i , and the Stoner factor, $(1 - I)^{-1}$ used as the fitting parameters (Table 2). The phase coherence time, τ_c , is a fundamental parameter that can be obtained from the magnetoresistivity data. The values of the fitting parameters D , τ_{so} , F are those derived from the electrical resistivity fit. These parameters are given in Table 1. The T_c 's and $\rho(290$ K)'s are

Table 2 Values of the hydrogen concentration, x , the inelastic scattering time, $\tau_i(4.2$ K), the density of states at Fermi-level, $N(E_F)$, and the Stoner factor, $(1 - I)^{-1}$ obtained from the magnetoresistivity data.

| x | $\tau_i(4.2$ K) | $N(E_F)$ | $(1 - I)^{-1}$ |
|--|---------------------------|--|----------------|
| ± 0.002 | ± 0.1 10^{-11} s | ± 0.1 states $\text{eV}^{-1} \text{at.}^{-1}$ | ± 0.05 |
| $(\text{Zr}_{80}\text{Ni}_{20})_{1-x}\text{H}_x$ | | | |
| 0 | 3.6 | 2.61 | 1 |
| 0.03 | 4.1 | 2.59 | 1.1 |
| 0.05 | 4.2 | 2.54 | 1.25 |
| 0.11 | 4.5 | 2.48 | 1.3 |
| $(\text{Zr}_{80}\text{Co}_{20})_{1-x}\text{H}_x$ | | | |
| 0 | 3.4 | 2.49 | 1 |
| 0.05 | 4.0 | 2.42 | 3.5 |
| 0.11 | 4.2 | 2.36 | 3.6 |

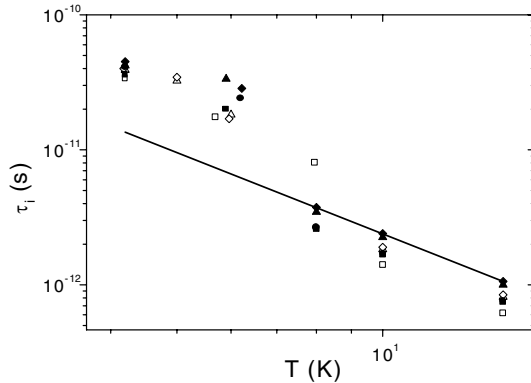


Fig. 6 The dephasing time, τ_i , as a function of temperature in hydrogen doped $(\text{Zr}_{80}\text{Ni}_{20})_{1-x}\text{H}_x$ [$x = 0$ (■), 0.03 (●), 0.05 (▲), 0.11 (◆)] and $(\text{Zr}_{80}\text{Co}_{20})_{1-x}\text{H}_x$ [$x = 0$ (□), 0.05 (△), 0.11 (◇)] metallic glasses. The solid line corresponds to a T^{-2} decrease.

those determined experimentally (Table 1). The orbital contribution, Eq. (5), is about 0.4% of the measured magnetoresistivities at the largest magnetic field used. The contribution to the magnetoresistivity from the spin-splitting term, Eq. (6) is greatly reduced in our system by the spin-orbit scattering and it amounts to about 0.04% of the measured magnetoresistivities at the largest magnetic field used.

The absolute value of τ_i can give us a better understanding of the dominant relaxation mechanisms. The temperature dependence of τ_i for hydrogen doped $(\text{Zr}_{80}3\text{d}_{20})_{1-x}\text{H}_x$ (3d = Ni, Co; $x \leq 0.11$) metallic glasses is shown in Fig. 6. The temperature dependence of τ_i closely follows a T^{-2} in the temperature range from 10 K to 110 K and is associated with electron–phonon relaxation processes. Below 10 K a more complicated temperature dependence of τ_i is observed, which has its origin in the electron–electron inelastic time due to the Maki–Thompson interaction, as well as the temperature-independent spin scattering at magnetic impurities. The difference between the inelastic scattering time, τ_i (4.2 K), obtained from the electrical resistivity fits and the magnetoresistivity fits can be explained by the τ_i (4.2 K) saturation at low temperature (Fig. 6). We can compare the observed values of τ_i with the ones calculated from theoretical predictions.

Takayama has calculated the inelastic scattering time due to the electron–phonon scattering [18]

$$\tau_{i(e-ph)} = \frac{k_F l \hbar^2 \omega_D}{2\pi^2 \lambda (k_B T)^2}, \quad (7)$$

with λ the electron–phonon coupling constant, k_B is the Boltzmann constant, k_F is the Fermi vector, l is the electron mean-free path and ω_D the Debye frequency.

If we use the known values of parameters for the $(\text{Zr}_{80}\text{Ni}_{20})_{1-x}\text{H}_x$ metallic glass: $x = 0$; $\lambda = 0.55$, $k_F = 1.35 \times 10^{10} \text{ m}^{-1}$, $l = 3.35 \times 10^{-10} \text{ m}$, $T = 4.2 \text{ K}$ and $\omega_D = 2.09 \times 10^{13} \text{ s}^{-1}$ and for $x = 0.11$; $\lambda = 0.5$, $k_F = 1.34 \times 10^{10} \text{ m}^{-1}$, $l = 3.2 \times 10^{-10} \text{ m}$, $T = 4.2 \text{ K}$ and $\omega_D = 2.19 \times 10^{13} \text{ s}^{-1}$ we obtain from Eq. (7) $\tau_{i(e-ph)} = 2.9 \times 10^{-11} \text{ s}$, for $x = 0$, and $\tau_{i(e-ph)} = 3.16 \times 10^{-11} \text{ s}$, for $x = 0.11$. Thus, we can conclude that hydrogen enhances the phase coherent time $\tau_{i(e-ph)}$ by providing additional centres for elastic scattering. The enhancement of $\tau_{i(e-ph)}$ is consistent with the observed (Table 2) increase of the inelastic scattering time, τ_i , with the dopant.

The Stoner factor, $(1 - I)^{-1}$, increases with increasing hydrogen concentrations (e.g., $(1 - I)^{-1} = 1$ for the undoped sample whereas $(1 - I)^{-1} = 3.6$ for $(\text{Zr}_{80}\text{Co}_{20})_{0.89}\text{H}_{0.11}$). The enhancement of the Stoner factor is larger in hydrogen doped $(\text{Zr}_{80}\text{Co}_{20})_{1-x}\text{H}_x$ than in $(\text{Zr}_{80}\text{Ni}_{20})_{1-x}\text{H}_x$ metallic glasses.

4 Conclusion

We have analysed the electrical resistivity, the superconducting transition temperature and the magnetoresistivity results as a function of hydrogen concentration in $(\text{Zr}_{80}3\text{d}_{20})_{1-x}\text{H}_x$ (3d = Co, Ni) metallic glasses.

The resistivity increase of $(\text{Zr}_{80}\text{3d}_{20})_{1-x}\text{H}_x$ is partly caused by the decrease of the density of d-states at the Fermi level, $N(E_F)$, and partly by the observed decrease of the electron diffusion constant, D , (Table 1).

The hydrogen dopant lowers T_c and broadens the superconducting transition region of the resistivity. The effect of hydrogen on the lowering of T_c is through the decrease of the Zr 4d-density of states at the Fermi level and enhancement of disorder.

The temperature dependence of the resistivity and magnetoresistivity have been analyzed using theoretical models of weak-localisation and electron–electron interaction in disordered three-dimensional conductors. Measurements in the magnetic field show positive anomalous magnetoresistance which can be interpreted as being due to WL in the presence of strong spin-orbit scattering and Maki-Thompson, MT, fluctuations. It has been found that both the spin-orbit and MT contributions are strongly suppressed with the dopant. At the same time, hydrogen increases the inelastic scattering time, τ_i .

References

- [1] H. Fukuyama and T. Hoshino, *J. Phys. Soc. Jpn.* **50**, 2131 (1981).
- [2] B. L. Al'tshuler, A. G. Aronov, A. I. Larkin, and D. E. Khmel'nitzkii, *Sov. Phys. JETP* **54**, 411 (1981).
- [3] P. A. Lee and T. V. Ramakrishnan, *Phys. Rev. B* **26**, 4009 (1982).
- [4] B. L. Al'tshuler and A. G. Aronov, in: *Electron–electron interaction in disordered systems*, edited by A. L. Efros and M. Pollak (North-Holland, Amsterdam, 1985), pp. 1 and 109.
- [5] R. Gupta, A. Gupta, A. K. Nigam, and G. Chandra, *J. Alloys Compd.* **326**, 275 (2001).
- [6] A. K. Majumdar, *J. Magn. Magn. Mater.* **263**, 26 (2003).
- [7] C. Papastaikoudis, M. Giannouri, G. Apostolopoulos, and I. Papastaikoudi, *Physica B* **284–288**, 1938 (2000).
- [8] M. Aprili, J. Lesueur, L. Dumoulin, and P. Nedellec, *Solid State Commun.* **102**, 41 (1997).
- [9] L. G. Aslamazov and A. I. Larkin, *Phys. Lett. A* **26**, 238 (1968).
- [10] K. Maki, *Theor. Phys.* **39**, 897 (1968).
R. S. Thompson, *Phys. Rev. B* **1**, 327 (1970).
- [11] D. V. Baxter, R. Richter, M. L. Trudeau, R. W. Cochrane, and J. O. Strom-Olsen, *J. Phys. (Paris)* **50**, 1673 (1989).
- [12] A. I. Larkin, *Pis'ma Zh. Eksp. Teor. Fiz.* **31**, 239 (1980).
- [13] K. Samwer and W. L. Johnson, *Phys. Rev. B* **28**, 2907 (1983).
- [14] I. Kokanović, B. Leontić, and J. Lukatela, *Fizika A* **4**, 615 (1995).
- [15] U. Mizutani, S. Ohta, and T. Matsuda, *J. Phys. Soc. Jpn.* **54**, 3406 (1985).
- [16] R. Zehringer, P. Oelhafen, H. J. Guntherodt, Y. Yamada, and U. Mizutani, *Mater. Sci. Eng.* **99**, 253 (1988).
- [17] I. Kokanović, B. Leontić, J. Lukatela, and K. Zadro, *J. Magn. Magn. Mater.* **188**, 138 (1998).
- [18] H. Takayama, *Z. Phys.* **263**, 329 (1973).